Statics and dynamics of quasi one-dimensional Bose–Einstein condensate in harmonic and dimple trap

2016 Laser Phys. 26 065501

(http://iopscience.iop.org/1555-6611/26/6/065501)

IOP Publishing | Astro Ltd Laser Physics

Laser Phys. **26** (2016) 065501 (10pp) doi:10.1088/1054-660X/26/6/065501

Statics and dynamics of quasi one-dimensional Bose–Einstein condensate in harmonic and dimple trap

Javed Akram[1,2] **and Axel Pelster**[3]

[1] Institute für Theoretische Physik, Freie Universität Berlin, Arnimallee 14, 14195 Berlin, Germany
[2] Department of Physics, COMSATS, Institute of Information Technology Islamabad, Pakistan
[3] Fachbereich Physik und Forschungszentrum OPTIMAS, Technische Universität Kaiserslautern, Germany

E-mail: javedakram@daad-alumni.de and axel.pelster@physik.uni-kl.de

Received 4 October 2015, revised 13 April 2016
Accepted for publication 14 April 2016
Published 6 May 2016

Abstract

We investigate a quasi one-dimensional ^{87}Rb Bose–Einstein condensate in a harmonic trap with an additional dimple trap (dT) in the center. Within a zero-temperature Gross–Pitaevskii mean-field description we provide a one-dimensional physical intuitive model, which we solve by both a time-independent variational approach and numerical calculations. With this we obtain at first equilibrium results for the emerging condensate wave function which reveal that a dimple trap potential induces a bump or a dip in case of a red- or a blue-detuned Gaussian laser beam, respectively. Afterwards, we investigate how this dT induced bump/dip-imprint upon the condensate wave function evolves for two quench scenarios. At first we consider the generic case that the harmonic confinement is released. During the resulting time-of-flight expansion it turns out that the dT induced bump in the condensate wave function remains present, whereas the dip starts decaying after a characteristic time scale which decreases with increasing blue-detuned dT depth. Secondly, once the red- or blue-detuned dT is switched off, we find that bright shock-waves or gray/dark bi-soliton trains emerge which oscillate within the harmonic confinement with a characteristic frequency.

Keywords: Bose–Einstein condensate, bright shock-waves, solitons

(Some figures may appear in colour only in the online journal)

1. Introduction

The ability to manipulate and trap atoms with laser light has had a tremendous development in many fields of physics. The very first experimental success of trapping 500 sodium atoms for several seconds in the tight focus of a Gaussian red-detuned laser beam occurred in 1986 [1]. The physical mechanism behind such an optical dipole trap is the electric dipole interaction of the trapped polarized atoms with the intense laser light, which is far detuned from the nearest optical transition of the atoms. They are hence largely independent from magnetic sublevels of the confined atoms, in contrast to a magneto-optical trap (MOT) which can only trap atoms with a certain internal state [2, 3]. The so called dimple trap (dT) is nothing but a small tight optical dipole trap [4–6]. Cooling and trapping of atoms with these dT's has a strong impact on the study of the Bose–Einstein condensates [7, 8], the observation of long decay times for atoms in their ground state [9], and the research of trapping other atomic species or molecules [10].

A straightforward method for realizing a dT is to rely on the potential created by a freely propagating laser beam. The detuning of the laser frequency versus the atomic resonances determines whether the laser is red/blue-detuned, i.e. the laser frequency is below/above the atomic resonance frequency, respectively [2]. The red-detuned dT was particularly used for realizing matter wave traps [11–13] in the focus of a Gaussian laser beam. On the other hand, the blue-detuned Gaussian

laser beam was used in optical waveguides [14–19], where the creation of repulsive potentials was demonstrated by using Laguerre–Gaussian laser beam [20–25]. A focused or well-collimated Gaussian laser beam with a large red-detuning [26] or a dark hollow laser beam with a large blue-detuning [27] were used to form 3D optical dipole trap's, which can be widely applied to the accurate, non-contact manipulation and control of cold atoms [28–30].

In this paper, we will focus on studying neutral ^{87}Rb atoms within a quasi one-dimensional harmonic trap with an additional dimple trap. Experimentally, a highly elongated quasi-1D regime can be reached by tightly confining the atoms in the radial direction, effectively freezing-out the transverse dynamics [31–38]. It is worth mentioning that, when the transverse length scales are of the order of or less than the atomic interaction length, the one-dimensional system can only be described within the Tonks–Girardeau or within the super-Tonks–Girardeau regime [39–41], which is experimentally realizable near a confinement-induced resonance [42–44]. On the other hand, when the transverse confinement is larger than the atomic interaction strength, the underlying three-dimensional Gross–Pitaevskii equation (GPE) can be reduced to an effective quasi 1D model [45]. In one spatial dimension (1D) this equation is well-known, for instance, to feature bright and dark solitons for attractive and repulsive s-wave scattering lengths, respectively [46–50]. Many experiments investigate the collision of two Bose–Einstein condensates where the celebrated matter-wave interference pattern appears [51] or shock-waves are generated [52]. For lower collisional energies, the repulsive interaction energy becomes significant, and the interference pattern evolves into an array of gray solitons [53–59]. Furthermore, dark solitons can be created by manipulating the condensate density using external potentials [60–62].

This work is organized as follows: in section 2, we start with the model which describes the dynamical evolution of a quasi-1D Bose–Einstein condensate (BEC) in a magneto-optical trap with an additional red/blue-detuned dimple trap in the center. Afterwards in section 3, we justify a Thomas–Fermi approximation for the condensate wave function and compare it with numerical results. With this we show that the dT induces a bump or a dip upon the condensate wave function depending on whether dT laser beam is red- or blue-detuned. Subsequently, in section 4, we discuss the dynamics of the dT induced bump/dip-imprint upon the condensate wave function for two quench scenarios. After having released the trap, the resulting time-of-flight expansion shows that the dT induced imprint remains conserved for a red-detuned dT but decreases for a blue-detuned dT. Furthermore, when the initial red/blue-detuned dT is switched off, we observe the emergence of bright shock-waves or gray/dark bi-soliton trains. Finally, in the section 5 we summarize our findings for the proposed quasi-1D harmonically confined BEC with an additional dimple trap in the center in view of a possible experimental realization.

2. Quasi 1D model

We consider here a BEC, which is confined by a harmonic trap with an additional dT potential in the center and is described by the corresponding one-dimensional Gross–Pitaevskii equation

$$\mathrm{i}\hbar\frac{\partial}{\partial t}\psi(z,t) = \left\{-\frac{\hbar^2}{2m_\mathrm{B}}\frac{\partial^2}{\partial z^2} + \frac{m_\mathrm{B}\omega_z^2}{2}z^2 + U\mathrm{e}^{-\frac{2z^2}{W_{0z}^2}} + G_\mathrm{B}\|\psi(z,t)\|^2\right\}\psi(z,t). \tag{1}$$

Here the two-particle interaction strength reads $G_\mathrm{B} = 2N_\mathrm{B}a_\mathrm{B}\hbar\omega_\mathrm{r}$, where N_B denotes the number of bosonic atoms and ω_r is the transversal trap frequency. In case of ^{87}Rb atoms, for instance, the s-wave scattering length is $a_\mathrm{B} = 94.7\,\mathrm{a}_0$ with the Bohr radius a_0. In the following, we consider the experimentally realistic trap frequencies $\omega_\mathrm{r} = 2\pi\times 160\,\mathrm{Hz} \gg \omega_z = 2\pi\times 6.8\,\mathrm{Hz}$ [3], so we have a cigar-shaped condensate, where the oscillator lengths amount to the values $l_\mathrm{r} = 0.84\,\mu\mathrm{m} \ll l_z = 4.12\,\mu\mathrm{m}$. Thus, the MOT provides, indeed, a quasi one-dimensional setting due to $a_\mathrm{B} \ll l_\mathrm{r} \ll l_z$. The Gaussian potential in equation (1) stems from the dT and has a depth $U = 2U_0P/(\pi W_{0z}\sqrt{W_{0x}^2 + 2l_\mathrm{r}^2})$ [63–65], which depends on the power P of the Gaussian laser beam as well as its widths along the x-axis $W_{0x} = 1.1\,\mu\mathrm{m}$ and along the z-axis $W_{0z} = 3.2\,\mu\mathrm{m}$, which are about ten times smaller than the corresponding ones used in [3]. Furthermore, the detuning $\Delta = \omega - \omega_\mathrm{A}$ not only changes the absolute value of the dT depth but also its sign. For red detuning, i.e. when the laser frequency ω is smaller than the atomic frequency ω_A, the dT is negative and the atoms are sucked into the dT potential. In the opposite case of blue detuning the atoms are repelled from the dT potential. Thus, the dT induces an imprint on the BEC wave function, which can be either a bump for red detuning or a dip for blue detuning. In order to make equation (1) dimensionless, we introduce the dimensionless time as $\tilde{t} = \omega_z t$, the dimensionless coordinate $\tilde{z} = z/l_z$, and the dimensionless wave function $\tilde{\psi} = \psi/\sqrt{l_z}$. With this equation (1) can be written in the form

$$\mathrm{i}\frac{\partial}{\partial\tilde{t}}\tilde{\psi}(\tilde{z},\tilde{t}) = \left\{-\frac{1}{2}\frac{\partial^2}{\partial\tilde{z}^2} + \frac{1}{2}\tilde{z}^2 + \tilde{U}\mathrm{e}^{-\frac{\tilde{z}^2}{\tilde{\alpha}^2}} + \tilde{G}_\mathrm{B}\times\|\tilde{\psi}(\tilde{z},\tilde{t})\|^2\right\}\tilde{\psi}(\tilde{z},\tilde{t}), \tag{2}$$

where we have $\tilde{G}_\mathrm{B} = 2N_\mathrm{B}\omega_\mathrm{r}a_\mathrm{B}/(\omega_z l_z)$ and $\tilde{U} = U/(\hbar\omega_z)$. For the above mentioned experimental parameters and $N_\mathrm{B} = 20\times 10^4$ atoms of ^{87}Rb, we obtain the dimensionless couplings constant $\tilde{G}_\mathrm{B} = 11435.9$. Furthermore, the typical dT depth $|U|/k_\mathrm{B} = 210\,\mathrm{nK}$ yields the dimensionless value $|U| = 643.83$, and $\tilde{\alpha} = W_{0z}/(\sqrt{2}\,l_z) = 0.548$ represents the ratio of the width of the dT potential along the z-axis and the longitudinal harmonic oscillator length. From here on, we will drop all tildes for simplicity.

3. dT induced bump/dip-imprint upon stationary condensate wave function

In order to determine the dT induced imprint on the condensate wave function in equilibrium, we solve the 1DGPE (2)

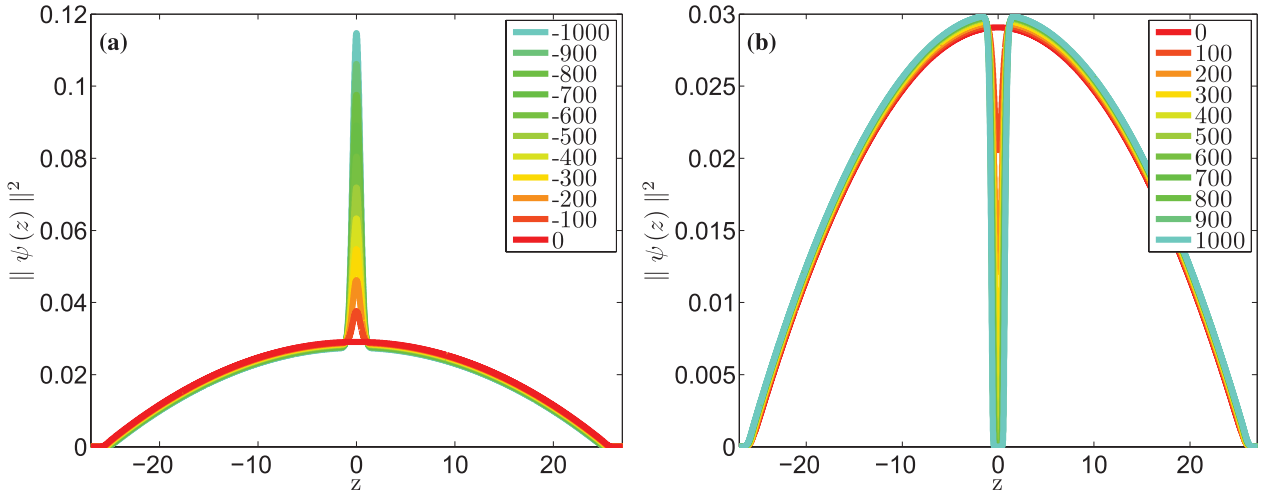

Figure 1. Numerical density profile of BEC for the experimental coupling constant value $G_B = 11435.9$ and for the dT depth U which increases from top to bottom according to the inlets. For (a) negative values of U, the bump in the condensate wave function decreases, whereas for (b) positive values the corresponding dip increases.

in imaginary time numerically by using the split-operator method [66, 67]. In this way we find that the dT-imprint leads to a bump/hole in the BEC density at the trap center for negative/positive values of U as shown in figure 1. For stronger red-detuned dT depth values the bump increases further, but for stronger blue-detuned dT the dip in the BEC density gets deeper and deeper until no more BEC atoms remain in the trap center. After this qualitative overview on the numerical results, we now work out an analytic approach for describing this red/blue-detuned dT induced bump/dip on the BEC density in a more quantitative way. To this end we present two arguments why the seminal Thomas–Fermi (TF) approximation is also applicable in our context.

At first we provide a rough estimate in the case of an absent dT, i.e. $U = 0$, so the BEC density is characterized by the TF profile $\psi(z) = \sqrt{(\mu - z^2/2)/G_B}\,\Theta(\mu - z^2/2)$, where the Heaviside function Θ prevents the density to become negative. Thus, the Tomas–Fermi radius $\sqrt{2\mu}$ follows from the dimensionless chemical potential μ, which is determined by normalization to be $\mu = \frac{1}{2}\left(\frac{3}{2}\right)^{2/3}(G_B)^{2/3}$. As the red/blue-detuned dT is supposed to be inserted at the trap center, we then calculate the dimensionless BEC coherence length ξ at the trap center. It is defined by comparing the kinetic energy $1/2\xi^2$ with the interaction energy in the trap center, which is given by μ. For the above mentioned experimental parameters this yields the dimensionless BEC coherence length $\xi = 0.038$, which is about 14.4 times smaller than the dT width $\alpha = 0.548$. This indicates that the dT induced imprint upon the BEC wavefunction occurs on a length scale which is much larger than its coherence length, so the TF approximation seems to be reasonable even in the presence of the red/blue-detuned dT.

In view of a more quantitative justification for the applicability of the Thomas–Fermi approximation, figure 2 presents the numerical result how the interaction energy E_{int}, the potential energy E_{pot}, and the kinetic energy E_{kin} of the condensate wave function change with increasing or decreasing the

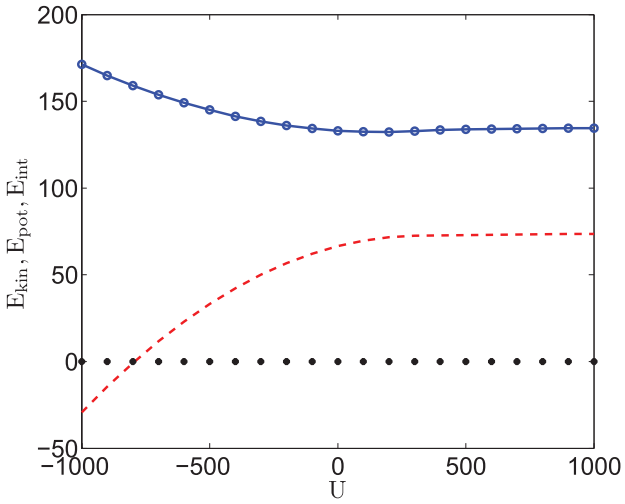

Figure 2. Here, we plotted E_{int} (blue-line circles), E_{pot} (red dashed line) and E_{kin} (black circles) versus U from solving 1DGPE (2).

red/blue-detuned dT depth U. We read off that the inequality $(E_{pot} + E_{int})/E_{kin} \gg 1$ holds within the whole region of interest for U, so the TF approximation seems to be, indeed, valid. Note that the maximal value of this energy ratio occurs for $U = 0$ and amounts to 7.5×10^4, which is of the order of the number of particles.

These results motivate to investigate in the following the TF approximation in more detail for non-zero red/blue-detuned dT depth U. To this end we use for the condensate wave function the ansatz $\psi(z,t) = \psi(z)e^{-i\mu t}$, insert it into the 1DGPE (2), and neglect the kinetic energy term, which yields the density profile

$$\psi(z) = \sqrt{\frac{1}{G_B}\left(\mu - \frac{z^2}{2} - Ue^{-\frac{z^2}{\alpha^2}}\right)}\,\Theta\left(\mu - \frac{z^2}{2} - Ue^{-\frac{z^2}{\alpha^2}}\right). \quad (3)$$

In view of the normalization $\int_{-\infty}^{+\infty} \|\psi(z)\|^2 dz = 1$, which fixes the chemical potential μ, we have to determine the

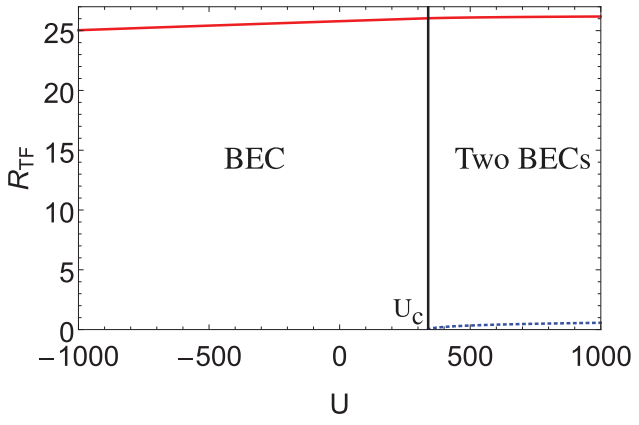

Figure 3. Outer Thomas–Fermi radius R_{TF1} (red solid) and inner Thomas–Fermi radius R_{TF2} (blue dashed) versus dimple trap depth U. BEC divides into two parts above $U_c \approx 339.5$.

Thomas–Fermi radii R_{TF} from the condition that the condensate wave function vanishes:

$$\mu = \frac{R_{\mathrm{TF}}^2}{2} + U\mathrm{e}^{-\frac{R_{\mathrm{TF}}^2}{\alpha^2}}. \tag{4}$$

As can be read off from figure 1(b) the number of solutions of equation (4) changes for increasing dT depth at a critical value U_c which we determine as follows. We put $\mu_c = U_c$ and utilize the normalization condition $2\int_0^{R_{\mathrm{TF}}} \|\psi(z)\|^2 \mathrm{d}z = 1$ with assuming one TF radius $R_{\mathrm{TF}} \approx \sqrt{2\mu}$. This yields the implicit equation

$$U_c = \frac{1}{2}\left(\frac{3}{2}\right)^{\frac{2}{3}}(G_{\mathrm{B}} + \sqrt{\pi}\,\alpha U_c)^{\frac{2}{3}}, \tag{5}$$

which results in $U_c \approx 339.5$ for the experimental coupling constant $G_{\mathrm{B}} = 11435.9$, which compares well with the value $U_c \approx 342$ determined from solving 1DGPE (2). In the case that U is smaller than U_c equation (4) defines only the cloud radius R_{TF1}. But for the case $U > U_c$ the dT drills a hole in the center of the ^{87}Rb condensate, so it divides into two parts. Thus, we have then apart from the outer cloud radius R_{TF1} also an inner cloud radius R_{TF2}. With this the normalization condition $2\int_{R_{\mathrm{TF2}}}^{R_{\mathrm{TF1}}} \|\psi(z)\|^2 \mathrm{d}z = 1$ yields

$$\mu(R_{\mathrm{TF1}} - R_{\mathrm{TF2}}) - \frac{1}{6}(R_{\mathrm{TF1}}^3 - R_{\mathrm{TF2}}^3) = \frac{G_{\mathrm{B}}}{2} + \frac{\sqrt{\pi}\,\alpha U}{2}\left[\mathrm{Erf}\left(\frac{R_{\mathrm{TF1}}}{\alpha}\right) - \mathrm{Erf}\left(\frac{R_{\mathrm{TF2}}}{\alpha}\right)\right], \tag{6}$$

where $\mathrm{Erf}(y) = \frac{2}{\sqrt{\pi}}\int_0^y \mathrm{e}^{-x^2}\mathrm{d}x$ denotes the error function. In case of $U \leqslant U_c$ the inner cloud radius R_{TF2} vanishes and the cloud radius is approximated via $R_{\mathrm{TF1}} \approx \sqrt{2\mu}$ due to equation (4) as it is much larger than the dimple trap width α. Thus, by using the approximation $\mathrm{Erf}(R_{\mathrm{TF1}}/\alpha) \approx 1$ for $R_{\mathrm{TF1}}/\alpha \gg 0$, the chemical potential is determined explicitly from

$$\mu \approx \frac{1}{2}\left(\frac{3}{2}\right)^{2/3}\left(G_{\mathrm{B}} + \sqrt{\pi}\,\alpha U\right)^{2/3}, \quad U \leqslant U_c. \tag{7}$$

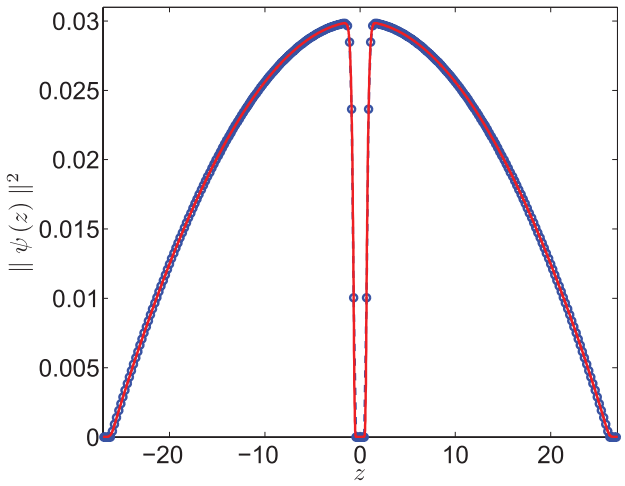

Figure 4. Condensate density for $U = 1000$ from solving 1DGPE (2) in imaginary time numerically (red) and from TF approximation (3) (blue-circles).

Provided that $U \geqslant U_c$, the inner cloud radius R_{TF2} has to be taken into account according to figure 1 and, due to the fact that $R_{\mathrm{TF2}}^2 \ll U$, we get from equation (4) the approximation $\mu \approx U\mathrm{e}^{-\frac{R_{\mathrm{TF2}}^2}{\alpha^2}}$, which reduces to

$$R_{\mathrm{TF2}} \approx \alpha\sqrt{\log\left(\frac{U}{\mu}\right)}. \tag{8}$$

Thus, we conclude that R_{TF2} vanishes, indeed, at U_c according to equations (5) and (7). With this we obtain from equation (6) that the chemical potential follows from solving

$$3\left[\sqrt{\pi}\,\alpha U + G_{\mathrm{B}} + 2\alpha\mu\sqrt{\log\left(\frac{U}{\mu}\right)}\right] \approx 3\sqrt{\pi}\,\alpha U \times \mathrm{Erf}\left(\sqrt{\log\left(\frac{U}{\mu}\right)}\right) + \alpha^3\log^{\frac{3}{2}}\left(\frac{U}{\mu}\right) + 4\sqrt{2}\,\mu^{3/2}, \; U \geqslant U_c. \tag{9}$$

Figure 3 shows the resulting outer and inner Thomas–Fermi radius as a function of the dT depth U. We read off that $R_{\mathrm{TF1}} \approx \sqrt{2\mu}$ remains approximately constant for $U \geqslant U_c$, so we conclude that the chemical potential μ is locked to its critical value $\mu_c \approx U_c = 339.5$. Furthermore, we note that the inner Thomas–Fermi radius R_{TF2} increases up to about 5.4α for the considered range of U.

Figure 4 compares the resulting TF condensate wave function (3) with a numerical solution of the 1DGPE (2) in imaginary time at $U = 1000$ and we read off that both agree quite well. Thus, our TF approximation describes the equilibrium properties of the condensate wave function in the presence of the red/blue-detuned dT even quantitatively correct. In view of a more detailed comparison, we characterize the red/blue-detuned dT induced imprint upon the condensate wave function $\psi(z)$ by the following two quantities. The first one is the hight/depth (HD) of the dT induced imprint

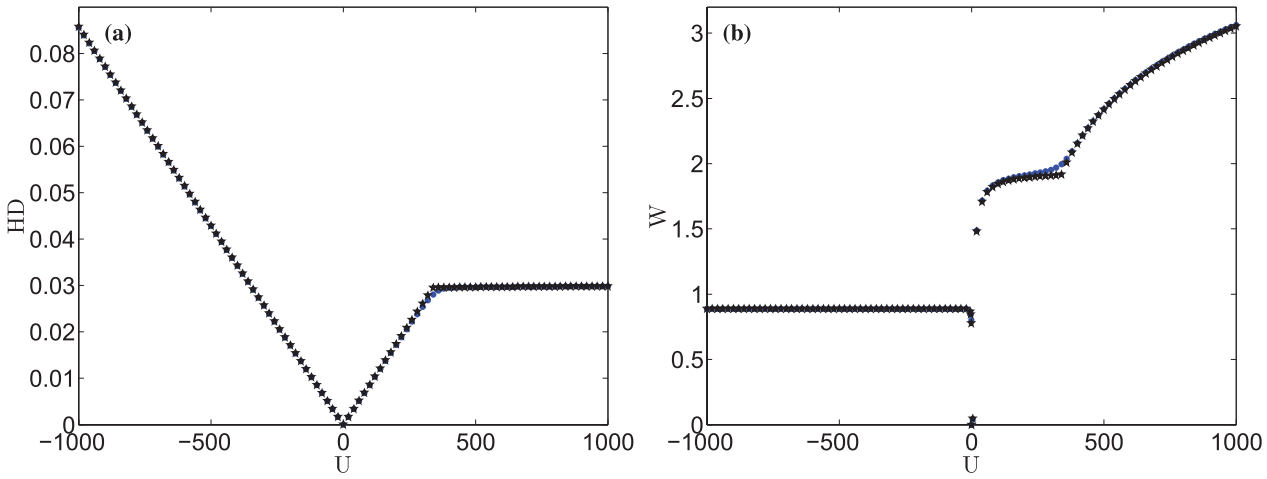

Figure 5. (a) Height/depth and (b) width of the dT induced bump/dip according to equations (10)–(12), versus the red/blue-detuned dT depth U for the experimental BEC coupling constant $G_{\mathrm{B}} = 11435.9$ calculated numerically by solving 1DGPE (2) in imaginary time (blue circles) and analytically (black stars) from the TF condensate wave function (3).

$$\mathrm{HD} = \begin{cases} \|\psi(0)\|_U^2 - \|\psi(0)\|_{U=0}^2 & U \leqslant 0 \\ \mathrm{Max}(\|\psi(z)\|_U^2) - \|\psi(0)\|_U^2 & U \geqslant 0 \end{cases} \tag{10}$$

and the second one is the red/blue-detuned dT induced imprint width W, which we define as follows. For $U \leqslant 0$ we use the full width half maximum

$$\|\psi(W/2)\|_U^2 = \frac{\|\psi(0)\|_U^2 + \|\psi(0)\|_{U=0}^2}{2} \quad U \leqslant 0, \tag{11}$$

whereas for $U > 0$ we define the equivalent width [68]:

$$W = \frac{2I_0 z_{\mathrm{Max}} - \int_{-z_{\mathrm{Max}}}^{z_{\mathrm{Max}}} \|\psi(z)\|_U^2 \,\mathrm{d}z}{I_0 - \|\psi(0)\|_U^2} \qquad U > 0, \tag{12}$$

where we have $I_0 = \mathrm{Max}(\|\psi(z)\|_U^2)$. Figure 5(a) shows the red/blue-detuned dT induced imprint height/depth as a function of U. At first, we read off that for $U = 0$, i.e. when we have not switched on the dT, bump/dip vanishes. Furthermore, in the range $U \leqslant U_{\mathrm{c}}$ we observe that height/depth of the dT induced imprint bump/dip changes linearly with U according to

$$\mathrm{HD} \approx \frac{|U|}{G_{\mathrm{B}}}. \tag{13}$$

In case of $U > U_{\mathrm{c}}$ height/depth of the dT induced imprint has approximately the constant value $\mathrm{HDc} = U_{\mathrm{c}}/G_{\mathrm{B}} \approx 0.029$ as follows from the TF wave function (3) and the above mentioned locking of the chemical potential to its critical value. Note that this constant value only slightly deviates from the corresponding numerical value $\mathrm{HDc} = 0.03$.

Correspondingly, figure 5(b) depicts the dimple trap induced width W as a function of U. From our TF approximation we obtain for the width transcendental formulas, which read in case of $U \leqslant 0$

$$\frac{W^2}{4} + 2U\mathrm{e}^{-\frac{W^2}{4\alpha^2}} - U + \frac{1}{2}\left(\frac{3}{2}\right)^{2/3}\left[G_{\mathrm{B}}^{2/3} - \left(G_{\mathrm{B}} + \sqrt{\pi}\,\alpha U\right)^{2/3}\right] = 0, \tag{14}$$

and for $U > \alpha^2/2$

$$W = \left\{2\alpha^3\sqrt{\log\left(\frac{2U}{\alpha^2}\right)}\left[2\log\left(\frac{2U}{\alpha^2}\right) + 3\right] - 6\sqrt{\pi}\,\alpha U \times \mathrm{Erf}\left(\sqrt{\log\left(\frac{2U}{\alpha^2}\right)}\right)\right\}/3\left[\alpha^2 + \alpha^2\log\left(\frac{2U}{\alpha^2}\right) - 2U\right]. \tag{15}$$

As shown in figure 5(b), for a red-detuned dT depth, the width remains approximately constant and is determined by the FWHM of the dimple Gaussian. Just before $U = 0$ the width W starts to decrease to zero. For a blue-detuned dT the width of the dip continuously increases with an intermediate plateau at U_{c} with the value $\mathrm{Wc} \approx 1.91$, which agrees well with the numerically obtained one $\mathrm{Wc} \approx 1.99$. After the critical blue-detuned laser beam strength U_{c} the width of the imprint of the dT on the condensate increases drastically according to figure 5(b), as more and more BEC atoms move away from the center of the condensate.

Note that the Thomas–Fermi approximation would break down when the dimensionless healing length ξ/l_z in the trap center would be larger than the dimensionless dimple trap width α. This is the case for several previous studies treating experimentally relevant localized dimples, which can well be modeled by Dirac delta potentials [69, 70].

4. Dimple trap induced imprint upon condensate dynamics

To this end we investigate two quench scenarios numerically in more detail. The first one is the standard time-of-flight (TOF) expansion after having switched off the harmonic trap when the amplitude of the red/blue-detuned dT is still present. In the second case we consider the inverted situation that the red/blue-detuned dT is suddenly switched off within a remaining harmonic confinement. This turns out to give rise to the emergence of bright shock-waves or bi-solitons trains, i.e. two trains of more than one soliton each, respectively.

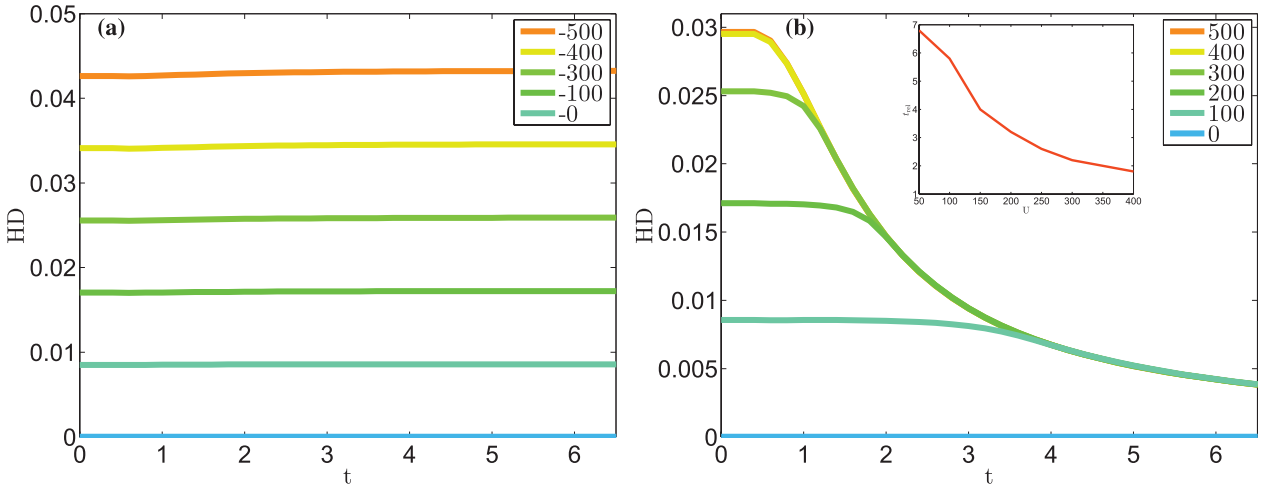

Figure 6. Height/depth of the dT induced imprint after having released the harmonic trap versus time for (a) increasing negative and (b) decreasing positive values of dT depth U from top to bottom. Inlet: relaxation time $t_{\rm rel}$ decreases with increasing U.

4.1. Time-of-flight expansion

Time-of-flight (TOF) absorption pictures represent an important diagnostic tool to analyze dilute quantum gases since the field's inception. By suddenly turning off the magnetic trap, the atom cloud expands in the presence of the dimple trap with a dynamics which is determined by both the momentum distribution of the atoms at the instance, when the confining potential is switched off, and by inter-atomic interactions [71, 72]. We have investigated the time-of-flight expansion dynamics of the BEC with the dT by solving numerically the 1DGPE (2) and analyzing the resulting evolution of the condensate wave function. It turns out that, despite the continuous broadening of the condensate density, its dT induced imprint remains qualitatively preserved both for red and blue-detuned dT. Therefore, we focus a more quantitative discussion upon the dynamics of the corresponding dT induced imprint height/depth and width.

For a red-detuned dT, it turns out that the bump height even remains constant in time. This is shown explicitly in figure 6(a), which roughly preserves its initial value at $t = 0$. This is due to the fact that a fraction of atoms remains trapped in the dimple trap while the rest of the cloud expands. This physical picture also explains the bump width, we even find that no significant changes do occur neither in time nor for varying U, therefore we do not present a corresponding figure. Note that the latter finding originates from figure 5(b), where the width is shown to be roughly constant for all dT depths.

Instead, in case of a blue-detuned dT, the dip decays after a characteristic time scale as shown in figure 6(b). Defining that relaxation time $t_{\rm rel}$ according to $\mathrm{HD}(t_{\rm rel}) = \mathrm{HD}(0)/2$, the inlet reveals that the dip relaxes with a shorter time scale for increasing blue-detuned dT depth U. These results are explained by the fact that an increasing blue-detuned dT potential pushes the expanding cloud even faster apart. This physical picture is confirmed by the dynamics of the dT induced imprint width shown in figure 7. At the beginning of TOF it remains at first constant and then increases gradually. This change of W occurs on the scale of the relaxation time of HD, which is depicted in figure 6(b).

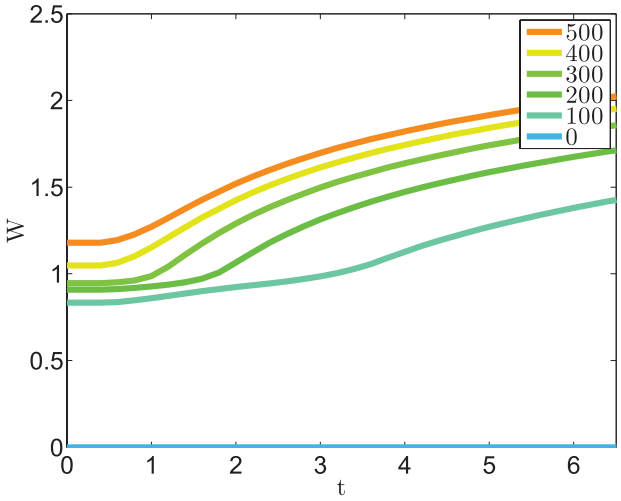

Figure 7. Width of the dT induced imprint after having released the trap versus time for decreasing positive values of dT depth U from top to bottom.

4.2. Wave packets versus solitons

Due to their quantum coherence, BECs exhibit rich and complex dynamic patterns, which range from the celebrated matter-wave interference of two colliding condensates [51, 52] over Faraday waves [73, 74] to the particle-like excitations of solitons [53–56, 59, 62, 75]. For our 1D model of a BEC with a harmonic and a dimple trap in the center, we investigated the dynamics of the condensate wave function which emerges after having switched off the dT. To this end, figure 8 depicts the resulting profile of density $n = |\psi|^2$ and phase $\phi = \tan^{-1}(\psi_{\rm Re}/\psi_{\rm Im})$ of the condensate wave function ψ at different instants of time. Both for an initial red- and blue-detuned dT, we observe that two excitations of the condensate are created at the dT position, which travel in opposite direction with the same center-of-mass speed, are reflected at the trap boundaries and then collide at the dT position. Furthermore, we find that these excitations qualitatively preserve their shape despite the collision and that the BEC wave

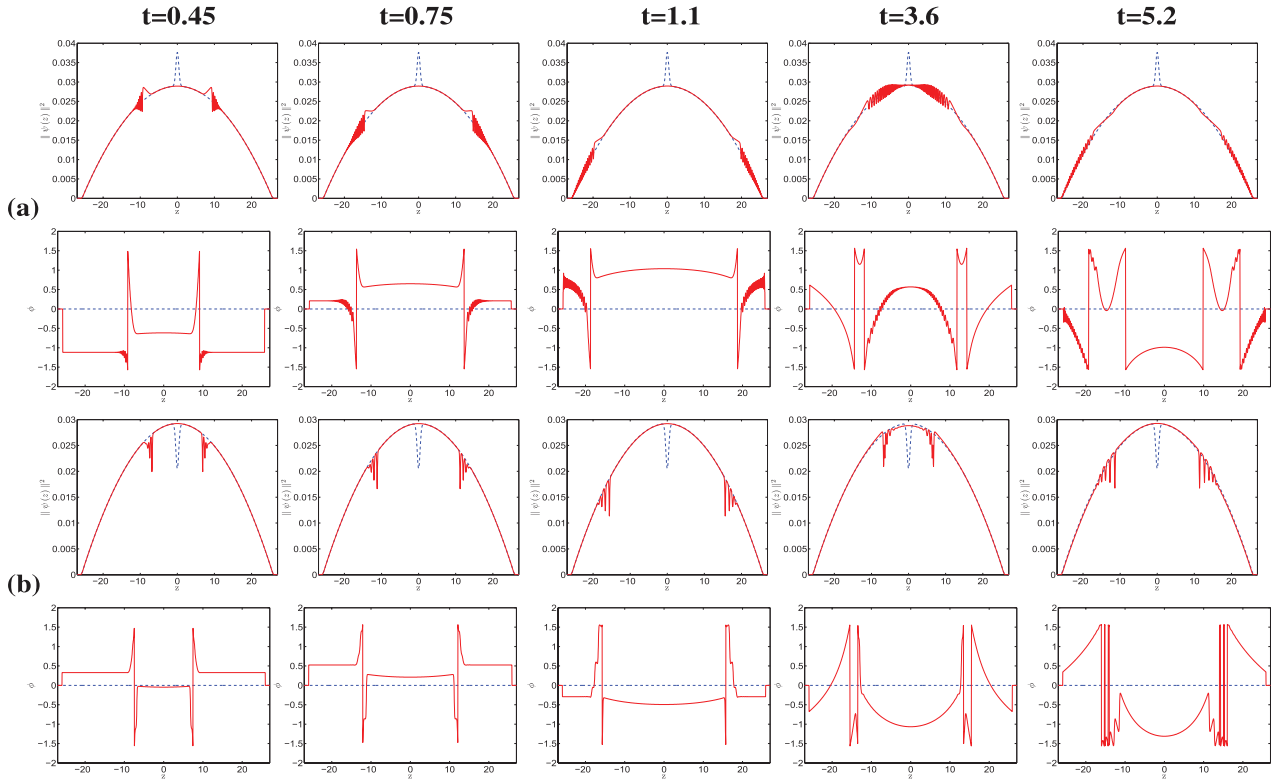

Figure 8. Density (phase) profile of BEC after having switched off the red/blue-detuned dT: in blue-dashed line at $t = 0$, and in red-solid line at $t = 0.45$ (1st column), $t = 0.75$ (2nd column), $t = 1.1$ (3rd column), $t = 3.6$ (4th column), and $t = 5.2$ (5th column) for (a) $U = -100$ and (b) $U = 100$.

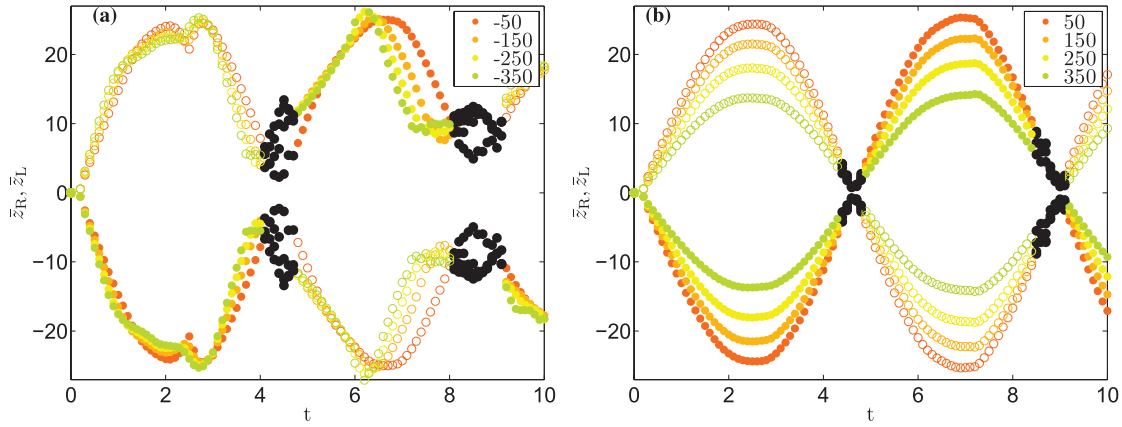

Figure 9. Center of mass positions of excitations $\bar{z}_{\mathrm{L}}$ (filled circles) and $\bar{z}_{\mathrm{R}}$ (empty circles) according to equation (16) versus time after having switched off the dT with increasing absolute value of the depth $|U|$ from top to bottom, for (a) red-detuning and (b) blue-detuning. Black filled circles represent the region of colliding excitations, where mean positions are not perfectly detectable.

function reveals characteristic phase slips between $-\pi/2$ and $\pi/2$. All these findings are not yet conclusive to decide whether these excitations represent wave packets in the absence of dispersion or solitons. Therefore, we investigate their dynamics in more detail, by determining their center-of-mass motion via

$$\bar{z}_{\mathrm{L,R}}(t) = \frac{\int_{-\infty,0}^{0,\infty} z(\|\psi(z,t)\|_U^2 - \|\psi(z,t)\|_{U=0}^2)\mathrm{d}z}{\int_{-\infty,0}^{0,\infty}(\|\psi(z,t)\|_U^2 - \|\psi(z,t)\|_{U=0}^2)\mathrm{d}z}, \quad (16)$$

which are plotted in figure 9. Note that the mean positions $\bar{z}_{\mathrm{L}}$ and $\bar{z}_{\mathrm{R}}$ of the excitations are uncertain in the region where they collide. Nevertheless figure 9 demonstrates that the excitations oscillate with the frequency $\Omega = 2\pi \times 4.87$ Hz irrespective of sign and size of U. As we have assumed the trap frequency $\omega_{\mathrm{z}} = 2\pi \times 6.8$ Hz, we obtain the ratio $\Omega/\omega_{\mathrm{z}} \approx 0.72$, which is quite close to $\Omega/\omega_{\mathrm{z}} = 1/\sqrt{2} \approx 0.707$.

Despite these similarities of the cases of an initial red and blue-detuned dT, we observe one significant difference. Whereas the oscillation amplitudes of the excitations do not depend on the value of the initial $U < 0$ according to

figure 9(a), we find decreasing oscillation amplitudes of the excitations with increasing the initial $U > 0$ in figure 9(b). The latter amplitude dependence on the initial condition is characteristic for gray/dark solitons according to [55]. Indeed, for an increasing dT potential the gray soliton acquires a larger depth, which corresponds to a smaller velocity, so its oscillation amplitude is reduced. This particle-like interpretation of the excitations is also confirmed by the other theoretical prediction of [55] that gray/dark solitons oscillate in a harmonic confinement with the frequency $\Omega/\omega_z = 1/\sqrt{2}$, which was already confirmed in Hamburg experiment [62] and in Heidelberg experiment [76] and is also seen in figure 9(b).

Conversely, for an initial red-detuned dT the excitations can not be identified with bright solitons as the dynamics is governed by a GPE with a repulsive two-particle interaction. Here the excitations have to be interpreted as wave packets which move without any dispersion as follows from a Bogoliubov dispersion relation and the smallness of the coherence length. Thus, for $U < 0$ the excitations propagate like sound waves in the BEC [51] and, within a TF approximation, their center-of-mass motion is described by the evolution equation [77]

$$\frac{\mathrm{d}z(t)}{\mathrm{d}t} = \sqrt{\mu - \frac{z^2(t)}{2}}\,. \tag{17}$$

Solving (17) with the initial condition $z(0) = 0$ yields the result $z(t) = \sqrt{2\mu}\,\sin t/\sqrt{2}$. Thus, we read off that the oscillation amplitude coincides with the TF radius and that the dimensionless oscillation frequency turns out to be $1/\sqrt{2}$ in agreement with figure 9(a).

Thus, we conclude that switching off the red/blue-detuned dT leads to physically different situations. For an initial red-detuned dT, we generate wave packets which correspond to white shock waves [78], whereas for the corresponding blue-detuned case bi-soliton trains emerge [53, 58, 79], due to the collision of the two divided parts of the condensate. Note that it can be shown in our system that gray bi-solitons trains are generated for a partially divided BEC, i.e. $U < U_c$. On the other hand the dark bi-solitons trains turn out to be only generated for $U \geqslant U_c$, where the BEC is well divided into two parts equilibrium.

5. Summary and conclusion

In the present work we studied within a quasi 1D model both analytically and numerically how a dimple trap in the center of a harmonically trapped BEC affects the condensate wave function. At first, we showed for the equilibrium properties of the system that the Thomas–Fermi approximation agrees quantitatively with numerical solutions of the underlying 1D Gross–Pitaevskii equation. For an increasing red-detuned dT depth, it turns out for the induced bump that the height decreases linearly, whereas the width remains approximately constant. In contrast to that we found for an increasing blue-detuned dT that depth and width of the induced dip initially increase. Beyond a critical value U_c, the BEC even divided into two parts and, if U is increased beyond U_c, the dT induced imprint yields a condensate wave function whose width increases further, although the dip height/depth remains constant. Afterwards, we investigated the dT induced bump/dip upon the condensate dynamics for two quench scenarios.

At first, we considered the release of the harmonic confinement, which leads to a time-of-flight expansion and found that the dT induced imprint remains conserved for a red-detuned dT but decreases in the blue-detuned case. This result suggests that it might be experimentally easier to observe the bump for a red-detuned dT. On the other hand, in an experiment one has to take into account that inelastic collisions lead to two- and three-body losses of the condensate atoms [80, 81]. As such inelastic collisions are enhanced for a higher BEC density, they play a vital role for a red-detuned dT, when the condensate density has a bump at the dT position, but are negligible for the blue-detuned dT with the dip in the BEC wave-function. Thus, a more realistic description of the experiment needs to consider the loss of condensate atoms by adding damping terms to the 1DGPE (2), which are of the form $\mathrm{i}\Upsilon_2\|\tilde{\Psi}(\tilde{z})\|^2$ and $\mathrm{i}\Upsilon_3\|\tilde{\Psi}(\tilde{z})\|^4$, where the positive constants Υ_2 and Υ_3 denote two- and three-body loss rates, respectively. We note that these additional terms may have nontrivial effects on the dT properties [82].

In addition, we analyzed the condensate dynamics after having switching off the red/blue-detuned dT. This case turned out to be an interesting laboratory in order to study the physical similarities and differences of bright shock-waves and gray/dark bi-soliton trains, which emerge for an initial red- and blue-detuned dT, respectively. The astonishing observation, that the oscillation frequencies of both the bright shock-waves and the bi-soliton trains coincide, is presumably an artifact of the harmonic confinement. Thus, it might be rewarding to further investigate these different dynamical features also in anharmonic confinements [83–85]. Additionally, we have also found that the generation of gray/dark bi-soliton trains is a generic phenomenon on collisions of partially/fully divided BEC, respectively, and the partially/fully divided BEC is strongly depending upon the equilibrium values of the dimple trap depth.

Acknowledgment

We thank J Anglin, A Balaž, T Bush, H Ott, E Santos, and A Widera for insightful comments. Furthermore, we gratefully acknowledge financial support from the German Academic Exchange Service (DAAD). This work was also supported in part by the German-Brazilian DAAD-CAPES program under the project name ‘Dynamics of Bose–Einstein Condensates Induced by Modulation of System Parameters’ and by the German Research Foundation (DFG) via the Collaborative Research Center SFB/TR49 ‘Condensed Matter Systems with Variable Many-Body Interactions’.

References

[1] Chu S, Bjorkholm J E, Ashkin A and Cable A 1986 *Phys. Rev. Lett.* **57** 314
[2] Grimm R, Weidemüller M and Ovchinnikov Y 2000 *Adv. At. Mol. Opt. Phys.* **42** 95

[3] Garrett M C, Ratnapala A, van Ooijen E D, Vale C J, Weegink K, Schnelle S K, Vainio O, Heckenberg N R, Rubinsztein-Dunlop H and Davis M J 2011 *Phys. Rev.* A **83** 013630
[4] Ma Z Y, Foot C J and Cornish S L 2004 *J. Phys. B: At. Mol. Opt. Phys.* **37** 3187
[5] Comparat D, Fioretti A, Stern G, Dimova E, Tolra B L and Pillet P 2006 *Phys. Rev.* A **73** 043410
[6] Jacob D, Mimoun E, Sarlo L D, Weitz M, Dalibard J and Gerbier F 2011 *New J. Phys.* **13** 065022
[7] Stenger J, Inouye S, Stamper-Kurn D M, Miesner H J, Chikkatur A P and Ketterle W 1998 *Nature* **396** 345
[8] Stellmer S, Pasquiou B, Grimm R and Schreck F 2013 *Phys. Rev. Lett.* **110** 263003
[9] Davidson N, Jin Lee H, Adams C S, Kasevich M and Chu S 1995 *Phys. Rev. Lett.* **74** 1311
[10] Weinstein J D, deCarvalho R, Guillet T, Friedrich B and Doyle J M 1998 *Nature* **395** 148
[11] Ashkin A 1970 *Phys. Rev. Lett.* **24** 156
[12] Stamper-Kurn D M, Andrews M R, Chikkatur A P, Inouye S, Miesner H J, Stenger J and Ketterle W 1998 *Phys. Rev. Lett.* **80** 2027
[13] González-Férez R, Iñarrea M, Salas J P and Schmelcher P 2014 *Phys. Rev.* E **90** 062919
[14] Xu X, Minogin V G, Lee K, Wang Y and Jhe W 1999 *Phys. Rev.* A **60** 4796
[15] Song Y, Milam D and Hill W T 1999 *Opt. Lett.* **24** 1805
[16] Xu X, Kim K, Jhe W and Kwon N 2001 *Phys. Rev.* A **63** 063401
[17] Noh H R, Xu X and Jhe W 2002 *Adv. At. Mol. Opt. Phys.* **48** 153
[18] Bongs K, Burger S, Dettmer S, Hellweg D, Arlt J, Ertmer W and Sengstock K 2001 *Phys. Rev.* A **63** 031602
[19] Yin J 2006 *Phys. Rep.* **430** 1
[20] Gallatin G M and Gould P L 1991 *J. Opt. Soc. Am.* B **8** 502
[21] Söding J, Grimm R and Ovchinnikov Y 1995 *Opt. Commun.* **119** 652
[22] Kuga T, Torii Y, Shiokawa N, Hirano T, Shimizu Y and Sasada H 1997 *Phys. Rev. Lett.* **78** 4713
[23] Kuppens S, Rauner M, Schiffer M, Sengstock K, Ertmer W, van Dorsselaer F E and Nienhuis G 1998 *Phys. Rev.* A **58** 3068
[24] Yin J and Zhu Y 1998 *Opt. Commun.* **152** 421
[25] Webster S A, Hechenblaikner G, Hopkins S A, Arlt J and Foot C J 2000 *J. Phys. B: At. Mol. Opt. Phys.* **33** 4149
[26] Metcalf H and van der Straten P 1994 *Phys. Rep.* **244** 203
[27] Yin J, Gao W and Zhu Y 2003 *Prog. Opt.* **45** 119
[28] Barrett M D, Sauer J A and Chapman M S 2001 *Phys. Rev. Lett.* **87** 010404
[29] Gustavson T L, Chikkatur A P, Leanhardt A E, Görlitz A, Gupta S, Pritchard D E and Ketterle W 2001 *Phys. Rev. Lett.* **88** 020401
[30] Akram J, Girodias B and Pelster A 2016 *J. Phys. B: At. Mol. Opt. Phys.* **49** 075302
[31] Görlitz A *et al* 2001 *Phys. Rev. Lett.* **87** 130402
[32] Moritz H, Stöferle T, Köhl M and Esslinger T 2003 *Phys. Rev. Lett.* **91** 250402
[33] Tolra B L, O'Hara K M, Huckans J H, Phillips W D, Rolston S L and Porto J V 2004 *Phys. Rev. Lett.* **92** 190401
[34] Hellweg D, Cacciapuoti L, Kottke M, Schulte T, Sengstock K, Ertmer W and Arlt J J 2003 *Phys. Rev. Lett.* **91** 010406
[35] Kinoshita T, Wenger T and Weiss D S 2005 *Phys. Rev. Lett.* **95** 190406
[36] Chuu C-S, Schreck F, Meyrath T P, Hanssen J L, Price G N and Raizen M G 2005 *Phys. Rev. Lett.* **95** 260403
[37] Hofferberth S, Lesanovsky I, Fischer B, Schumm T and Schmiedmayer J 2007 *Nature* **449** 324
[38] Eckart M, Walser R and Schleich W P 2008 *New J. Phys.* **10** 045024
[39] Olshanii M 1998 *Phys. Rev. Lett.* **81** 938
[40] Petrov D S, Shlyapnikov G V and Walraven J T M 2000 *Phys. Rev. Lett.* **85** 3745
[41] Bergeman T, Moore M G and Olshanii M 2003 *Phys. Rev. Lett.* **91** 163201
[42] Paredes B, Widera A, Murg V, Mandel O, Fölling S, Cirac I, Shlyapnikov G V, Hänsch T W and Bloch I 2004 *Nature* **429** 277
[43] Kinoshita T, Wenger T and Weiss D S 2004 *Science* **305** 1125
[44] Haller E, Gustavsson M, Mark M J, Danzl J G, Hart R, Pupillo G and Nägerl H-C 2009 *Science* **325** 1224
[45] Kamchatnov A 2004 *J. Exp. Theor. Phys.* **98** 908
[46] Radouani A 2004 *Phys. Rev.* A **70** 013602
[47] Kevrekidis P G, Frantzeskakis D and Carretero-González R 2008 *Emergent Nonlinear Phenomena in Bose–Einstein Condensates* (Berlin: Springer)
[48] Frantzeskakis D J 2010 *J. Phys. A: Math. Theor.* **43** 213001
[49] Cuevas J, Kevrekidis P G, Malomed B A, Dyke P and Hulet R G 2013 *New J. Phys.* **15** 063006
[50] Akram J and Pelster A 2016 *Phys. Rev.* A **93** 033610
[51] Andrews M R, Townsend C G, Miesner H J, Durfee D S, Kurn D M and Ketterle W 1997 *Science* **275** 637
[52] Dutton Z, Budde M, Slowe C and Hau L V 2001 *Science* **293** 663
[53] Reinhardt W P and Clark C W 1997 *J. Phys. B: At. Mol. Opt. Phys.* **30** L785
[54] Scott T F, Ballagh R J and Burnett K 1998 *J. Phys. B: At. Mol. Opt. Phys.* **31** L329
[55] Busch T and Anglin J R 2000 *Phys. Rev. Lett.* **84** 2298
[56] Ruostekoski J, Kneer B, Schleich W P and Rempe G 2001 *Phys. Rev.* A **63** 043613
[57] Khaykovich L, Schreck F, Ferrari G, Bourdel T, Cubizolles J, Carr L D, Castin Y and Salomon C 2002 *Science* **296** 1290
[58] Strecker K E, Partridge G B, Truscott A G and Hulet R G 2002 *Nature* **417** 150
[59] Shomroni I, Lahoud E, Levy S and Steinhauer J 2009 *Nat. Phys.* **5** 193
[60] Burger S, Bongs K, Dettmer S, Ertmer W, Sengstock K, Sanpera A, Shlyapnikov G V and Lewenstein M 1999 *Phys. Rev. Lett.* **83** 5198
[61] Carr L D, Brand J, Burger S and Sanpera A 2001 *Phys. Rev.* A **63** 051601
[62] Becker C, Stellmer S, Soltan-Panahi P, Dorscher S, Baumert M, Richter E M, Kronjager J, Bongs K and Sengstock K 2008 *Nat. Phys.* **4** 496
[63] Milonni P and Eberly J 2010 *Laser Physics* (New York: Wiley)
[64] Saleh B and Teich M 2007 *Fundamentals of Photonics* (New York: Wiley)
[65] Akram J and Pelster A 2016 *Phys. Rev.* A **93** 023606
[66] Javanainen J and Ruostekoski J 2006 *J. Phys. A: Math. Gen.* **39** L179
[67] Vudragović D, Vidanović I, Balaž A, Muruganandam P and Adhikari S K 2012 *Comput. Phys. Commun.* **183** 2021
[68] Carroll B and Ostlie D 2007 *An Introduction to Modern Astrophysics* (Boston: Addison-Wesley)
[69] Uncu H, Tarhan D, Demiralp E and Müstecaplıoğlu O E 2007 *Phys. Rev.* A **76** 013618
[70] Goold J, O'Donoghue D and Busch T 2008 *J. Phys. B: At. Mol. Opt. Phys.* **41** 215301
[71] Mewes M O, Andrews M R, van Druten N J, Kurn D M, Durfee D S and Ketterle W 1996 *Phys. Rev. Lett.* **77** 416
[72] Inouye S, Pfau T, Gupta S, Chikkatur A P, Görlitz A, Pritchard D E and Ketterle W 1999 *Nature* **402** 641
[73] Engels P, Atherton C and Hoefer M A 2007 *Phys. Rev. Lett.* **98** 095301
[74] Balaž A and Nicolin A I 2012 *Phys. Rev.* A **85** 023613

[75] Kivshar Y S and Luther-Davies B 1998 *Phys. Rep.* **298** 81
[76] Weller A, Ronzheimer J P, Gross C, Esteve J, Oberthaler M K, Frantzeskakis D J, Theocharis G and Kevrekidis P G 2008 *Phys. Rev. Lett.* **101** 130401
[77] Damski B 2004 *Phys. Rev.* A **69** 043610
[78] Damski B 2006 *Phys. Rev.* A **73** 043601
[79] Al Khawaja U, Stoof H T C, Hulet R G, Strecker K E and Partridge G B 2002 *Phys. Rev. Lett.* **89** 200404
[80] Cornish S L, Claussen N R, Roberts J L, Cornell E A and Wieman C E 2000 *Phys. Rev. Lett.* **85** 1795
[81] Carretero-González R, Frantzeskakis D J and Kevrekidis P G 2008 *Nonlinearity* **21** R139
[82] Bao W and Jaksch D 2003 *SIAM J. Numer. Anal.* **41** 1406
[83] Bretin V, Stock S, Seurin Y and Dalibard J 2004 *Phys. Rev. Lett.* **92** 050403
[84] Kling S and Pelster A 2007 *Phys. Rev.* A **76** 023609
[85] Kling S and Pelster A 2009 *Laser Phys.* **19** 1072